- ***Linear-Electro Optic Effect in Cladding***: In the so-called silicon-organic hybrid (SOH) approach a conventional silicon-on-insulator waveguide is functionalized with an organic cladding material [15, 16]. This way critical fabrication steps can rely on high-yield processes based on CMOS fabrication technology of a silicon-on-insulator (SOI) wafer. The functional organic material can subsequently be deposited onto the wafer. Typical organic cladding materials may be highly-nonlinear $\chi^{(2)}$ chromophores [17, 18] for high-speed modulation [19] and difference-frequency generation [20], or liquid-crystals for low-voltage phase-shifters [21].

All three effects offer sufficiently fast modulation. The plasma effect though is limited by the lifetime of the charge carriers. In order to keep the plasma effect fast carriers are normally removed by applying a reverse biased field.

3. TRAVELLING WAVE OR LUMPED ELECTRODE APPROACH

Speed and power efficiency is also affected by the electrical contact. Two approaches are common:

- ***The traveling wave modulator,*** see Fig. 1(a), typically needs an electrical termination matched to the wave impedance in order to avoid reflections of RF waves that would interfere with the signal of the next bit. When a matched termination is used, the total power launched into the modulator is dissipated – in part by RF loss and capacitive loading, but eventually in the terminating resistor $R = 50\ \Omega$. The voltage amplitude across the modulator input terminal is $U_0 / 2$. For a DC-free rectangular drive voltage with a peak-to-peak open-circuit value $2U_0$, representing an alternating series of logical ones and logical zeros with a bitrate B_B, the energy consumption per bit can thus be approximated by $W_{\mathrm{bit}} = \left(2U_0/2\right)^2 / R / B_B$. Travelling wave modulators allow fast modulation if they are designed without any walk-off between electrical and optical signals [22].
- ***Lumped terminated & unterminated modulator:*** Lumped modulators are short and can be operated without terminating resistor. Many resonant modulator configurations are lumped modulators and are usually operated without termination. Examples are slow-light structures [23, 24] or ring resonators [25, 26]. Short non-resonant modulators can also be operated without termination [27]. As an additional advantage of the unterminated lumped modulator, the in-device modulation voltage (the voltage made available at the electrodes of the device) is about U_0, i.e., it nearly doubles as explained in Fig. 1(c) as compared to the terminated case, Fig. 1(b). The energy consumption of the modulator is then dominated by the capacitive load of the slot waveguide. For the lumped device, we estimate the power dissipation associated with charging and de-charging the total modulator capacitance $C_{\mathrm{MZM}} = 2\,C_{\mathrm{PM}}$ as seen by the coplanar waveguide (CPW) to be $W_{\mathrm{bit}} = C_{\mathrm{MZM}} \times U_{\mathrm{drive}}^2 / 4$. This again assumes equal probabilities of logical ones and zeros, and it takes into account that only transitions consume energy.

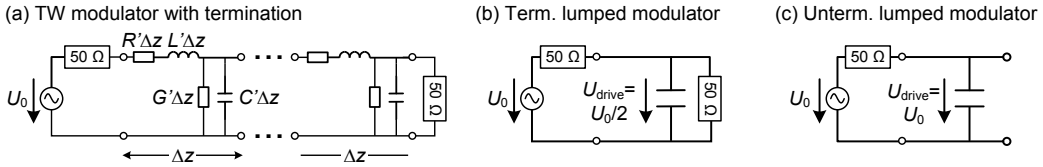

Figure 1. Equivalent circuit models of various modulator types. (a) Traveling-wave modulator. (b) Simplified model of a terminated lumped modulator. The drive voltage $U_0/2$ across the modulator input terminals is half the open-circuit source voltage U_0. The total RF power is dissipated by capacitive loading and by the 50 Ω termination. (c) Simplified model of an unterminated lumped modulator. The on-chip drive voltage U_0 equals the open-circuit voltage of the source. Power dissipation inside the modulator is dominated by capacitive loading. Residual power is reflected back to the source.

As an illustrative example, we recently characterized a 10 Gbit/s on-off keying SOH-modulator in a MZI configuration of 1.5 mm length with an 80 nm wide slot and $V_\pi L$ product of 3.0 Vmm [27]. The modulator can be operated in two ways:

- First, we operate the device with a 50 Ω termination and use a peak-to-peak drive voltage U_{drive} of 800 $\mathrm{mV_{pp}}$ (i.e., an amplitude of 400 $\mathrm{mV_p}$). The voltage V_π which is needed to switch a MZI modulator from minimum to maximum transmission was found to be 2.5 $\mathrm{V_{pp}}$ for high data rates. However, also smaller voltages suffice to get a clear and open eye. In our experiment the energy per bit thus was only 320 fJ when driving the modulator with 800 $\mathrm{mV_{pp}}$.
- Since the device was short and the bit-rate was chosen to be low, operation without a termination is possible. At this data rate the modulator acts as a lumped device. The capacitance of the MZI modulator was found to be $C_{\mathrm{MZM}} = 2\,C_{\mathrm{PM}} = 378\,\mathrm{fF}$, which resulted in an energy consumption of 60 fJ/bit.

4. OPTICAL WAVEGUIDE STRUCTURE AND INTERFEROMETER CONFIGURATION

The optical waveguide structure ultimately determines the performance of the modulator. It needs to be designed such that both the electrical and optical field are guided with a maximum overlap. Ideally, the applied voltage across the optical waveguide drops off within the optical waveguide such that the electrical field is highest.

For the realization of an efficient modulator within the silicon-organic hybrid approach we have decided for a strip-loaded slot waveguide structure, see Fig. 2(a). There are other structures that work well also [15], but the strip-loaded slot approach combines most of the advantages. In this approach the conductive silicon strip-loads connect the two rails of the slot waveguide with metal electrodes [15, 23]. Since the slot is typically only 100 nm wide, and both electrical and optical mode almost ideally overlap in the narrow slot, low voltages only are needed to induce a very high refractive index change in the nonlinear material of the slot. The structure has to be engineered for low losses, though. Unfortunately, the carriers of the doped strip-loads typically add to optical losses through free carrier absorption (FCA). For making the silicon strips sufficiently conductive without causing excessive optical losses it has been suggested to use gate-induced accumulation layers instead of ion-implantation [19].

To encode amplitude and phase on an optical signal we choose an IQ-interferometer configuration as depicted in Fig. 2(b).

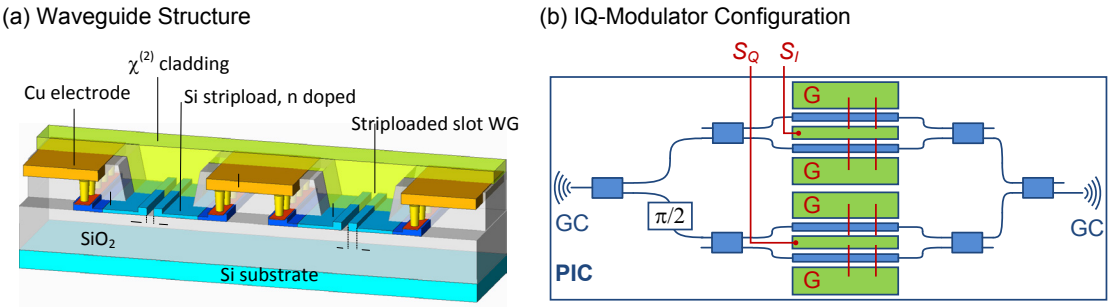

Figure 2: (a) Strip-loaded slot waveguide where metal electrodes are connected to the two rails of the slot waveguide by doped silicon strips (striploaded). Both, the modulating field and the optical mode are well confined to the slot. For efficient electro-optic modulation the slot needs to be filled with an adequate electro-optic material. (b) IQ-modulator configuration. More details on the Figures can be found in Ref. [28].

5. IQ MODULATOR PERFORMANCE

Finally, we demonstrate the performance of a recently published IQ modulator fabricated on the SOH platform. We show operation at 28 GBd with bit-rates up to 112 Gbit/s and extinction ratios of 26 dB. The device is 1.5 mm long and has a $V_\pi L$ product of 3.5 Vmm. This allows operation with an energy consumption of 640 fJ/bit. An in-depth description of both the structure and the experiment can be found in Ref. [28].

The frequency response of the modulator is shown in Fig. 3(a). The magenta line shows the frequency response of the modulator with an equalization of the frequency response in the receiver. A 3dB bandwidth of 21 GHz has been found. The blue line shows the frequency response of the modulator. It can be seen that the frequency response at first drops off sharply but then becomes extraordinarily flat towards higher frequencies. This flat response is in part responsible for the good performance at higher speed. The receiver transfer function for flattening the overall frequency response is separately plotted as a red curve in Fig.3(a) as well, and undoes the drop off of the frequency response at higher frequencies.

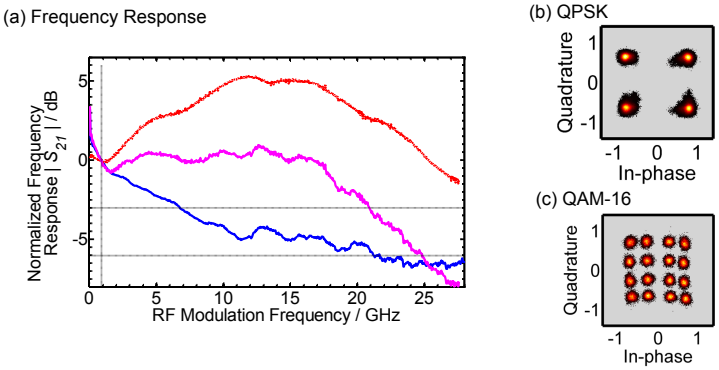

Figure 3: (a) Electro-optic frequency response S_{21} of our MZM. (Magenta line: frequency response of modulator+receiver; blue line: frequency response of modulator; red curve: frequency response of receiver). (b) SOH IQ modulator constellation diagrams for 28 GBd single polarization QPSK at 56 Gbit/s and (c) a 28 GBd single polarization 16-QAM signal with a total of 112 Gbit/s [28].

Finally, Fig. 3(b) shows the constellation diagram of a QPSK signal generated with the SOH modulator at a symbol rate of 28 GBd. This corresponds to a 56 Gbit/s signal. No equalization was used when these constellations were recorded. The symbols have a clear and distinct shape. The EVM was found to be 14.2% and

bit-error ratios are well below the detection limit of our setup. The constellation diagram in Fig. 3(c) shows how a 16-QAM signal can be generated with equalization at 28 GBd which corresponds to 112 Gbit/s. The symbols are round and distinct indicating a good signal quality. Measurements confirm that we are below the hard-decision FEC limit with a BER of 1.2×10^{-3}.

6. CONCLUSIONS

We review current silicon modulator concepts and discuss them with respect to speed and power consumption. We show that the silicon-organic hybrid approach offers a platform for ultra-compact modulators. We demonstrated operation from 10 GBd up to 28 GBd with an energy consumption of 60 fJ/bit at 10 Gbit/s up to 640 fJ/bit at 112 Gbit/s [27, 28].

Acknoweldgements
We acknowledge support by the EU-FP7 project SOFI, the BMBF joint project MISTRAL, the DFG Center for Functional Nanostructures (CFN), the Helmholtz International Research School on Teratronics (HIRST), the Karlsruhe School of Optics and Photonics (KSOP), and the Karlsruhe Nano-Micro Facility (KNMF).

References

[1] S. K. Selvaraja, W. Bogaerts, P. Absil, D. Van Thourhout, and R. Baets, "Record low-loss hybrid rib/wire waveguides for silicon photonic circuits," in *Group IV Photonics, 7th International conference, Proceedings*, 2010.
[2] T. Alasaarela, D. Korn, L. Alloatti, A. Säynätjoki, A. Tervonen, R. Palmer, J. Leuthold, W. Freude, and S. Honkanen, "Reduced propagation loss in silicon strip and slot waveguides coated by atomic layer deposition," *Opt. Express,* vol. 19, pp. 11529-11538, 06/06 2011.
[3] F. Xia, L. Sekaric, and Y. Vlasov, "Ultracompact optical buffers on a silicon chip," *Nat Photon,* vol. 1, pp. 65-71, 2007.
[4] L. Tsybeskov, D. J. Lockwood, and M. Ichikawa, "Silicon Photonics: CMOS Going Optical [Scanning the Issue]," *Proceedings of the Ieee,* vol. 97, pp. 1161-1165, 2009.
[5] M. Hochberg and T. Baehr-Jones, "Towards fabless silicon photonics," *Nat Photon,* vol. 4, pp. 492-494, 2010.
[6] L. P. David J. Lockwood, *Silicon Photonics: Components and Integration.* vol. II: Springer, 2011.
[7] G. T. Reed, G. Mashanovich, F. Y. Gardes, and D. J. Thomson, "Silicon optical modulators," *Nat Photon,* vol. 4, pp. 518-526, 2010.
[8] W. M. Green, M. J. Rooks, L. Sekaric, and Y. A. Vlasov, "Ultra-compact, low RF power, 10 Gb/s siliconMach-Zehnder modulator," *Opt. Express,* vol. 15, pp. 17106-17113, 12/10 2007.
[9] L. Liao, A. Liu, J. Basak, H. Nguyen, M. Paniccia, D. Rubin, Y. Chetrit, R. Cohen, and N. Izhaky, "40 Gbit/s silicon optical modulator for highspeed applications," *Electronics Letters,* vol. 43, 2007.
[10] D. J. Thomson, F. Y. Gardes, J. M. Fedeli, S. Zlatanovic, H. Youfang, B. P. P. Kuo, E. Myslivets, N. Alic, S. Radic, G. Z. Mashanovich, and G. T. Reed, "50-Gb/s Silicon Optical Modulator," *Photonics Technology Letters, IEEE,* vol. 24, pp. 234-236, 2012.
[11] P. Dong, X. Liu, C. Sethumadhavan, L. L. Buhl, R. Aroca, Y. Baeyens, and Y.-K. Chen, "224-Gb/s PDM-16-QAM Modulator and Receiver based on Silicon Photonic Integrated Circuits," 2013, p. PDP5C.6.
[12] R. S. Jacobsen, K. N. Andersen, P. I. Borel, J. Fage-Pedersen, L. H. Frandsen, O. Hansen, M. Kristensen, A. V. Lavrinenko, G. Moulin, H. Ou, C. Peucheret, B. Zsigri, and A. Bjarklev, "Strained silicon as a new electro-optic material," *Nature,* vol. 441, pp. 199-202, 05/11/print 2006.
[13] B. Chmielak, M. Waldow, C. Matheisen, C. Ripperda, J. Bolten, T. Wahlbrink, M. Nagel, F. Merget, and H. Kurz, "Pockels effect based fully integrated, strained silicon electro-optic modulator," *Opt. Express,* vol. 19, pp. 17212-17219, 08/29 2011.
[14] M. N. C. Matheisen, S. Sawallich, M. Waldo, B. Chmielak, T. Wahlbrink, J. Bolten, H. Kurz, "Locally induced electro-optic activity in silicon nanophotonic devices," *CLEO Europe 2013 - European Conference on Lasers and Electro-Optics,* 2013.
[15] J. Leuthold, W. Freude, J. M. Brosi, R. Baets, P. Dumon, I. Biaggio, M. L. Scimeca, F. Diederich, B. Frank, and C. Koos, "Silicon Organic Hybrid Technology: A Platform for Practical Nonlinear Optics," *Proceedings of the IEEE,* vol. 97, pp. 1304-1316, 2009.
[16] T. W. Baehr-Jones and M. J. Hochberg, "Polymer Silicon Hybrid Systems: A Platform for Practical Nonlinear Optics†," *The Journal of Physical Chemistry C,* vol. 112, pp. 8085-8090, 2008/05/01 2008.
[17] S.-S. Sun, L. R. Dalton, S.-S. Sun, and L. R. Dalton, *Introduction to Organic Electronic and Optoelectronic Materials and Devices (Optical Science and Engineering Series)*: CRC Press, Inc., 2008.
[18] P. G. L. Dalton, M. Jazbinsek, O. P. Kwon, P. A. Sullivan, *Organic Electro-Optics and Photonics*. in press: Cambridge University Press.
[19] L. Alloatti, D. Korn, R. Palmer, D. Hillerkuss, J. Li, A. Barklund, R. Dinu, J. Wieland, M. Fournier, J. Fedeli, H. Yu, W. Bogaerts, P. Dumon, R. Baets, C. Koos, W. Freude, and J. Leuthold, "42.7 Gbit/s electro-optic modulator in silicon technology," *Optics Express,* vol. 19, pp. 11841-11851, JUN 6 2011 2011.
[20] L. Alloatti, D. Korn, C. Weimann, C. Koos, W. Freude, and J. Leuthold, "Second-order nonlinear silicon-organic hybrid waveguides," *Optics Express,* vol. 20, pp. 20506-20515, AUG 27 2012 2012.
[21] J. Pfeifle, L. Alloatti, W. Freude, J. Leuthold, and C. Koos, "Silicon-organic hybrid phase shifter based on a slot waveguide with a liquid-crystal cladding," *Optics Express,* vol. 20, pp. 15359-15376, JUL 2 2012 2012.
[22] T. Baehr-Jones, R. Ding, Y. Liu, A. Ayazi, T. Pinguet, N. C. Harris, M. Streshinsky, P. Lee, Y. Zhang, A. E.-J. Lim, T.-Y. Liow, S. H.-G. Teo, G.-Q. Lo, and M. Hochberg, "Ultralow drive voltage silicon traveling-wave modulator," *Opt. Express,* vol. 20, pp. 12014-12020, 05/21 2012.
[23] J.-M. Brosi, C. Koos, L. C. Andreani, M. Waldow, J. Leuthold, and W. Freude, "High-speed low-voltage electro-optic modulator with a polymer-infiltrated silicon photonic crystal waveguide," *Optics Express,* vol. 16, pp. 4177-4191, MAR 17 2008 2008.
[24] J. H. Wülbern, A. Petrov, and M. Eich, "Electro-optical modulator in a polymerinfiltrated silicon slotted photonic crystal waveguide heterostructure resonator," *Opt. Express,* vol. 17, pp. 304-313, 01/05 2009.
[25] L. Chen, K. Preston, S. Manipatruni, and M. Lipson, "Integrated GHz silicon photonic interconnect with micrometer-scale modulators and detectors," *Opt. Express,* vol. 17, pp. 15248-15256, 08/17 2009.
[26] J. C. Rosenberg, W. M. Green, S. Assefa, T. Barwicz, M. Yang, S. M. Shank, and Y. A. Vlasov, "Low-Power 30 Gbps Silicon Microring Modulator," 2011, p. PDPB9.
[27] R. Palmer, L. Alloatti, D. Korn, P. C. Schindler, M. Baier, J. Bolten, T. Wahlbrink, M. Waldow, R. Dinu, W. Freude, C. Koos, and J. Leuthold, "Low Power Mach-Zehnder Modulator in Silicon-Organic Hybrid Technology," *Photonics Technology Letters, IEEE,* vol. PP, pp. 1-1, 2013.
[28] D. Korn, "112 Gbit/s silicon-organic hybrid (SOH) IQ modulator using the linear electro-optic effect," *Optics Express,* 2013.